Effect of Heat Input Conditions on Microstructure and Mechanical Properties of Friction-Stir-Welded Pure Copper

P. XUE, G.M. XIE, B.L. XIAO, Z.Y. MA, and L. GENG

Defect-free friction stir welds of 5-mm-thick pure copper plates were produced in relatively low heat input conditions. The characteristics of the microstructure and mechanical properties of the welded joints were investigated. The stir zone (SZ) exhibited equiaxed recrystallized grains, whose size decreased as the heat input was decreased. The percentage of high-angle grain boundaries (grain boundary misorientation angle >15 deg) in the SZ was quite high (90.2 to 94.5 pct) and increased as the heat input was increased. When the heat input was decreased, the percentage of the twin boundaries (TBs) dropped, and the number of the twin lamellas was reduced. Under a very low heat input condition, the typical characteristics of thermomechanically affected zone (TMAZ) were discernible; however, the TMAZ was characterized by a recrystallized grain structure at higher heat input conditions. The grains in the heat-affected zone (HAZ) were slightly coarsened compared to those in the parent material (PM), but the grain size varied a little under different parameters. The hardness of the SZ increased as the heat input was increased, and the lowest hardness appeared at the HAZs where the welds failed. The ultimate tensile strength (UTS) was similar to that of the PM under various heat input conditions, but the yield strength (YS) and elongation were lower. The YS increased as the lowest hardness value increased, and the elongation decreased due to the enhanced strain localization.

DOI: 10.1007/s11661-010-0254-y

I. INTRODUCTION

COPPER and its alloys have a wide range of applications due to their excellent properties, such as good ductility, corrosion resistance, electric conductivity, and thermal conductivity.[1] The welding of pure copper is extensively used in industrial production, such as in the nuclear industry and in vacuum devices.[2,3] Conventional fusion welding and braze welding have some obvious limitations. For fusion welding, a high heat input is required due to the good thermal conductibility of copper, resulting in remarkable grain coarsening with a wide heat-affected zone (HAZ) and a significant distortion with high residual stress. On the other hand, the strength of brazed copper joints is significantly lower than that of the fusion welded joints.[1]

Friction stir welding (FSW), invented by The Welding Institute of the United Kingdom in 1991, is an energy-efficient, environmentally friendly, and versatile joining technique.[4] The application of FSW has been reported in many industrial sectors, such as the production of ship panels, the frames of high speed railway, and the suspension arms of cars.[5] Extensive studies on the FSW of aluminum and its alloys have been reported, but limited research is available for copper.[6–13] As a solid-state welding process, FSW is performed at a temperature lower than the melting point of the materials. FSW involves a severe plastic deformation (SPD) process, and dynamic recrystallization (DRX) occurs in the stir zone (SZ) during the FSW process.[14] Therefore, the heat input during FSW of copper is much lower than that of conventional fusion welding methods, and high-quality copper joints with less distortion and higher strength can be obtained *via* FSW. Recently, the copper containment canisters for nuclear waste have been manufactured *via* FSW by the Swedish Nuclear Fuel and Waste Management Co.[6,7] Furthermore, Okamoto *et al.*[8] reported that the backing plates of copper alloy, used for the sputtering equipments, have been successfully welded by FSW.

Although the heat input for FSW is significantly lower than that for fusion welding, previous investigations on FSW of pure copper indicated that defect-free pure copper welds were achieved only at a lower traverse speed or higher rotation rate, *i.e.*, higher heat input conditions.[8–10] For example, Okamoto *et al.*[8] reported that 6-mm-thick copper plate was successfully welded at a rotation rate of 1300 rpm and a traverse speed of 170 mm/min. Similarly, Lee *et al.*[9] achieved defect-free joining of 4-mm-thick copper plate at a rotation rate of 1250 rpm and a traverse speed of 61 mm/min. The investigation by Hautala and Tiainen[10] also indicated that 5-mm-thick copper plates could be successfully welded only under rotation rates >800 rpm. However, in a previous study, we demonstrated that high-quality

P. XUE, Postgraduate, B.L. XIAO and Z.Y. MA, Professors, are with the Shenyang National Laboratory for Materials Science, Institute of Metal Research, Chinese Academy of Sciences, Shenyang 110016, P.R. China. Contact e-mail: zyma@imr.ac.cn G.M. XIE, Lecturer, is with State Key Laboratory of Rolling and Automation, Northeastern University, Shengyang 110004, P.R. China. L. GENG, Professor, is with the School of Materials Science and Engineering, Harbin Institute of Technology, Harbin 150001, P.R. China.

Manuscript submitted September 22, 2009.
Article published online June 9, 2010

FSW copper joints could be achieved under lower heat input conditions.[11] Recently, Liu *et al.*[12] obtained sound FSW copper joints 3 mm in thickness under a low heat input condition of 400 rpm–100 mm/min. It is well documented that the grain size of the welds could be reduced under lower heat input conditions, which usually results in the improvement of the mechanical properties.[8–12] Therefore, it is of practical importance to investigate the effect of heat input condition on the microstructure and mechanical properties of the FSW copper joints.

Certainly, the FSW heat input is also governed by other parameters. For example, Reynolds *et al.*[15,16] presented an input torque-based thermal simulation and studied the thermal history of FSW 7050Al alloy joints. However, torque is correlated to the complex conditions of the workpiece/tool interface, so it is difficult to get an accurate value.[16] For copper, no suitable thermal simulations can be used to evaluate the workpiece/tool interface conditions.

For the given tool geometry and plunge depth, the heat input is mainly determined by the rotation rate and traverse speed.[5] In this article, pure copper plates 5 mm in thickness were welded under a wide range of the welding parameters that generated different heat input conditions. The aim of this study is (a) to identify the possibility of obtaining defect-free FSW copper joints under lower heat input conditions and (b) to elucidate the effects of heat input condition on the microstructure and mechanical properties of the FSW copper joints.

II. EXPERIMENTAL

Commercially pure copper plate 5 mm in thickness with 1/2H condition was used in this study. The chemical composition was 0.1O-0.01S-0.01As-0.01Pb (wt pct). Plates 300 mm in length and 70 mm in width were welded along the rolling direction using a gantry FSW machine (China FSW Center). FSW was conducted at different heat input conditions: (1) a constant traverse speed of 50 mm/min with tool rotation rates of 400, 600, and 800 rpm, respectively; and (2) a constant rotation rate of 800 rpm with traverse speeds of 50, 100, and 200 mm/min, respectively. A tool with a shoulder 20 mm in diameter and a cylindrical threaded pin 6 mm in diameter and 4.7 mm in length was used. A tilting angle of 2.5 deg was used for all FSW processes and the plunge depth of the shoulder was controlled at ~0.2 mm.

Microstructural features were characterized by optical microscopy (OM) and transmission electron microscopy (TEM). The metallographic samples were cross sectioned perpendicular to the welding direction, polished, and then etched with a solution of 100 mL distilled water, 15 mL hydrochloric acid, and 2.5 g iron (III) chloride. TEM samples were prepared by means of double-jet electrolytic polishing in an electrolyte consisting of 25 pct (volume) alcohol, 25 pct phosphorus acid, and 50 pct deionized water at about 263 K (–10 °C). Crystallographic orientation for the SZ of the FSW joints was measured by the electron backscatter diffraction (EBSD) system (Oxford Instruments HKL, Hobro, Denmark, Channel 5 type). The EBSD specimens were machined on the transverse cross-sectional plane, as illustrated in Figure 1. The average grain sizes for EBSD and OM were measured automatically by the Channel 5 software and with the mean linear intercept method, respectively.

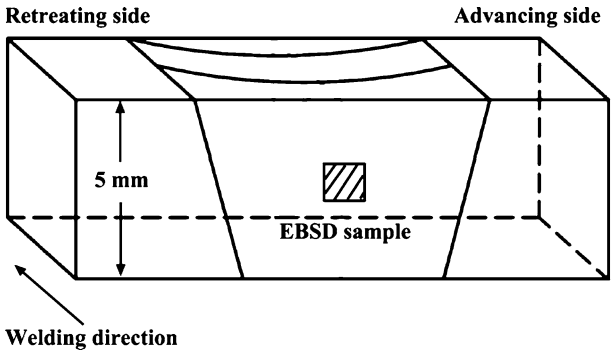

Fig. 1—Schematic illustration of EBSD sample location.

The microhardness of the FSW joints was measured along the midthickness of the plates with a 50-g load for 10 seconds by LECO*-LM247AT type Vickers-hardness machine. The tensile specimens with a gage length of 40 mm and a width of 10 mm were machined perpendicular to the FSW direction. In order to obtain the practical tensile properties of the welds, specimens with as-weld surfaces were used for the tensile test. The tensile test was carried out using a Zwick-Roell-type testing machine at an initial strain rate of 4.2×10^{-4} s^{-1}.

*LECO is a trademark of LECO Corporation, St. Joseph, MI.

III. RESULTS

A. *Influence of Heat Input Conditions on Microstructure Evolution*

The cross-sectional macrographs of the FSW copper joints under different welding parameters are shown in Figure 2. Defect-free welds were achieved under a wide rotation rate range of 400 to 800 rpm at a constant traverse speed of 50 mm/min and a wide traverse speed range of 50 to 200 mm/min at a constant rotation rate of 800 rpm. Based on the microstructural characterization, four distinct zones, *i.e.*, parent material (PM), SZ, thermomechanically affected zone (TMAZ), and HAZ, were usually identified in FSW joints,[5] as shown in Figure 2(e). It is noted that at a constant traverse speed of 50 mm/min, when the rotation rate was decreased from 800 to 400 rpm, the onion rings and boundary around the SZ became more and more obvious. Similarly, increasing the traverse speed from 50 to 200 mm/min at 800 rpm also made the onion rings and the boundary around the SZ clearer. It is well known that the heat input during the FSW process could be reduced

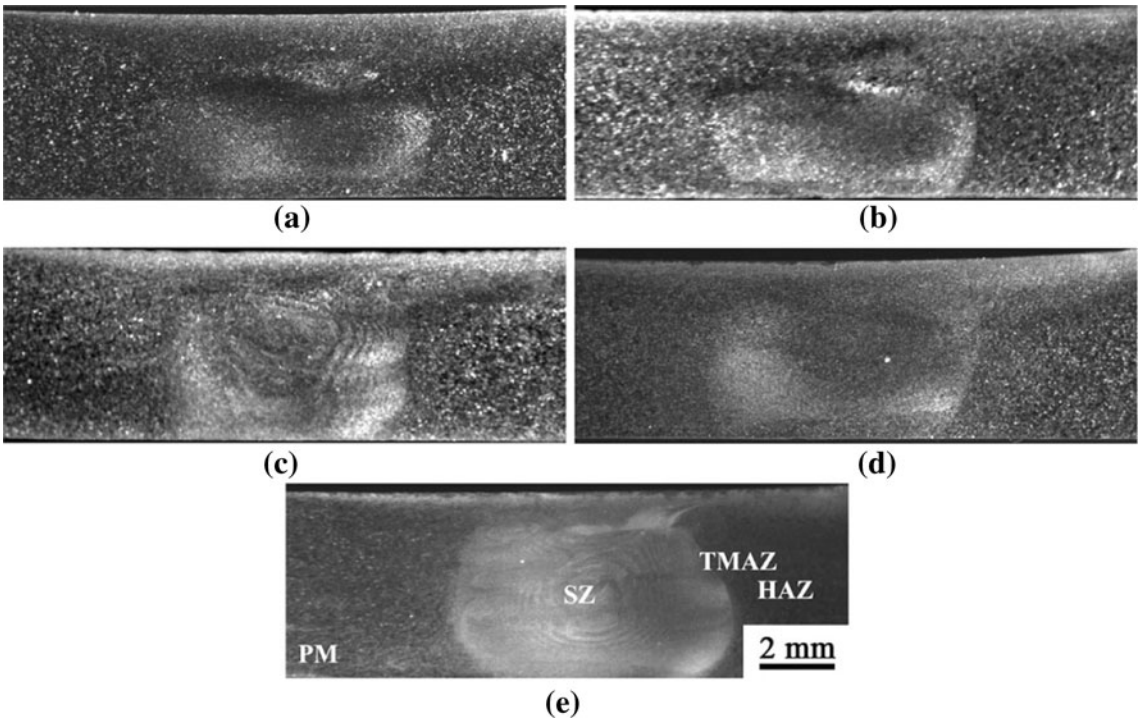

Fig. 2—Cross-sectional macrographs of FSW copper joints produced at traverse speeds of (*a*) 50 mm/min, (*b*) 100 mm/min, and (*c*) 200 mm/min (rotation rate: 800 rpm) and at rotation rates of (*d*) 600 rpm and (*e*) 400 rpm (traverse speed: 50 mm/min; the advancing side is on the right side).

by decreasing the rotation rate or increasing the traverse speed.[5] Therefore, the onion rings and the outline of the SZ could be clearly observed in the FSW copper joints at lower heat input conditions.

Figure 3 shows the microstructure of the PM and the SZ (center zone) under different welding parameters. The PM was characterized by coarse grains of ~18 μm with many annealing twins (Figure 3(a)). Compared to the PM, the SZ exhibited nearly equiaxed grain structure, and the size of the grains decreased significantly as the heat input was decreased, *i.e.*, decreasing rotation rate or increasing traverse speed. The average grain sizes of the PM and SZ under different parameters measured by the mean linear intercept method were shown in Table I.

The microstructures of the TMAZ at rotation rates of 800, 600, and 400 rpm at 50 mm/min are shown in Figures 4(a) through (c), respectively. As shown in Figure 4(a), under a high heat input condition of 800 rpm, the typical characteristics of the TMAZ that were observed in FSW Al alloy joints[5] were not discernible. Instead, the microstructure was characterized by equiaxed recrystallized grains. The average grain size in the TMAZ near the SZ was ~15 μm, which was smaller than that in the PM. Similarly, the TMAZ at 600 rpm also exhibited equiaxed grain structure, but the average grain size was reduced to ~12 μm. However, under a low heat input condition of 400 rpm, the TMAZ was characterized by the elongated grains distributed along the flow lines, which was the typical microstructure of the common TMAZ. Figure 4(d) shows the microstructure of the HAZ under the parameter of 400 rpm–50 mm/min. The grains were slightly coarsened compared to those in the PM. Under higher heat input conditions, the microstructure of the HAZ was similar to that obtained at 400 rpm–50 mm/min except for the slight increase in grain size, as shown in Table I.

The EBSD images of the PM and the SZ are presented in Figure 5, in which the black and white lines represent the high-angle grain boundaries (HAGBs, grain boundary misorientation angle >15 deg) and low-angle grain boundaries (LAGBs, 5 deg < grain boundary misorientation angle <15 deg), respectively. Similar to the observation by OM, the microstructure of the PM was characterized by coarse grains with many annealing twins. The SZ of the FSW joints exhibited nearly equiaxed grain structure, and the size of the grains decreased as the rotation rate was decreased. Furthermore, a nonuniform microstructure with coarse grain zones and fine grain zones was observed in the SZ at 400 rpm–50 mm/min (Figure 5(d)), and this was associated with the onion rings that consisted of alternating coarse grain bands and fine grain bands.[11] The average grain sizes of the PM and the SZ at 800, 600, and 400 rpm (50 mm/min), as determined by EBSD, were 16, 11, 9.3, and 3 μm, respectively. From the distribution maps of the grain boundary misorientation angle shown in Figure 6, the percentages of the HAGBs were 88.5, 94.5, 93.9, and 90.2 pct for the PM and the SZ at 800, 600, and 400 rpm (50 mm/min), respectively.

From the distribution maps of the grain boundary misorientation angle for the PM and the FSW samples (Figure 6), the largest peak appears at approximately 60 deg, which results from the $\Sigma 3$ coincident-site lattice

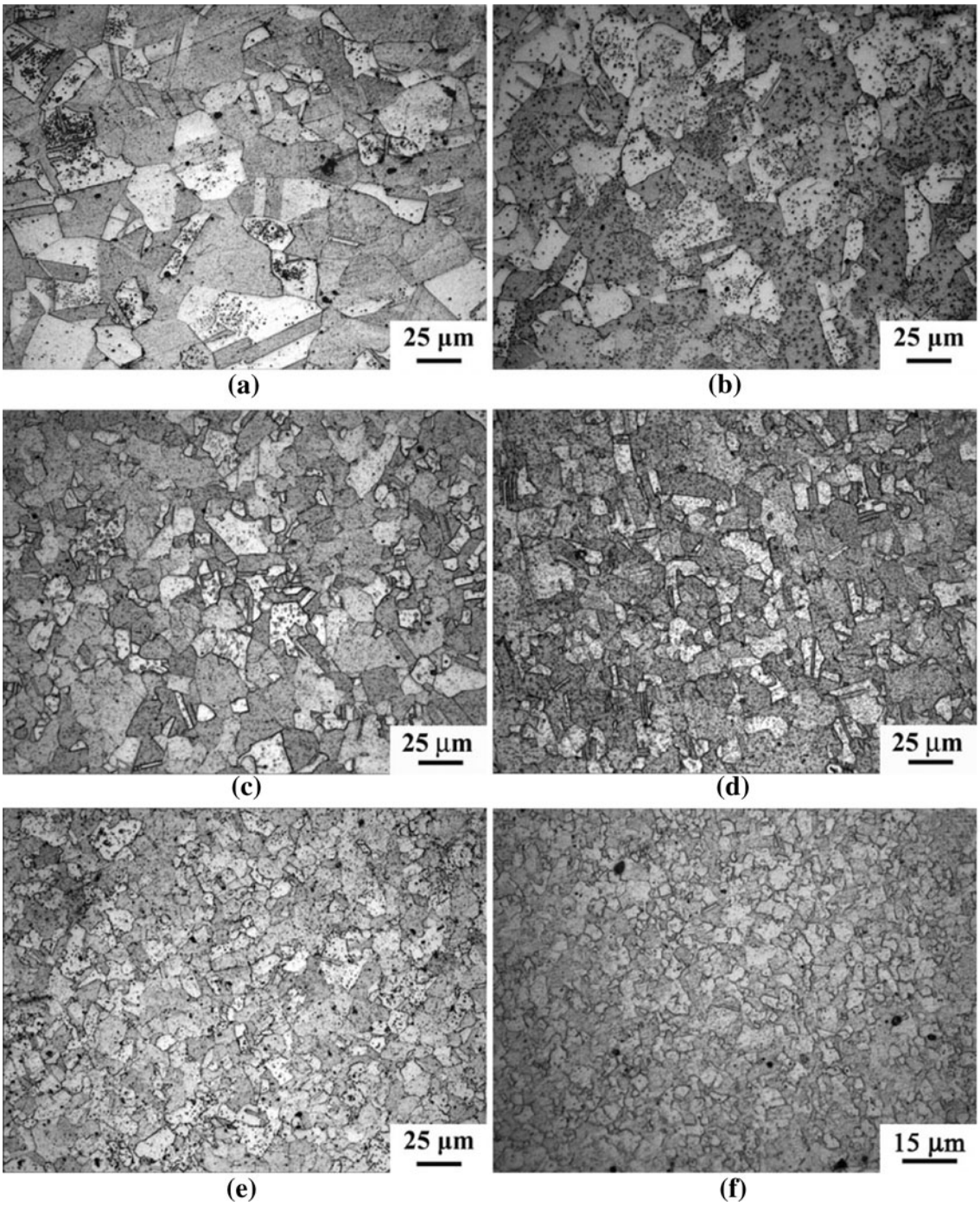

Fig. 3—Microstructures of (*a*) PM and SZ at traverse speed of (*b*) 50 mm/min, (*c*) 100 mm/min, and (*d*) 200 mm/min (rotation rate: 800 rpm) and rotation rate of (*e*) 600 rpm and (*f*) 400 rpm (traverse speed: 50 mm/min).

twin boundaries (TBs). Figure 7 shows the distributions of the Σ3 boundaries of the PM and the FSW samples. The percentages of the Σ3 boundaries for the PM and the FSW samples at 800, 600, and 400 rpm (50 mm/min) were determined to be 42.0, 37.3, 30.5, and 19.4 pct, respectively, by EBSD. It is noted from Figure 7 that at high heat input conditions of 600, 800 rpm–50 mm/min, similar to the PM, many twin lamellas consisting of nearly parallel boundaries could be observed. However, the twin lamellas were seldom observed at a very low heat input condition of 400 rpm–50 mm/min. Instead, individual TBs were frequently discerned, and the length was smaller due to the decreased grain size. A more detailed TEM microstructure of the different types of twins is shown in Figure 8. At a higher heat input condition of 800 rpm–50 mm/min, many typical annealing twin lamellas could be observed (Figure 8(a)). At a lower heat input condition of 400 rpm–50 mm/min,

Table I. Average Grain Size and Mechanical Properties of PM and FSW Pure Copper Joints

Materials	Grain Size (μm)		Strength (MPa)		El. (Pct)
	SZ	HAZ	UTS	YS	
PM, 1/2H	18	—	236.7	222.9	27.7
FSW, 800 rpm–50 mm/min	12	32	228.7	122.1	24.7
FSW, 800 rpm–100 mm/min	11	29	229.8	130.7	23.4
FSW, 800 rpm–200 mm/min	9	27	236.3	147.2	22.2
FSW, 600 rpm–50 mm/min	9	28	231.8	137.7	19.9
FSW, 400 rpm–50 mm/min	3.5	25	235.9	207.7	15.1

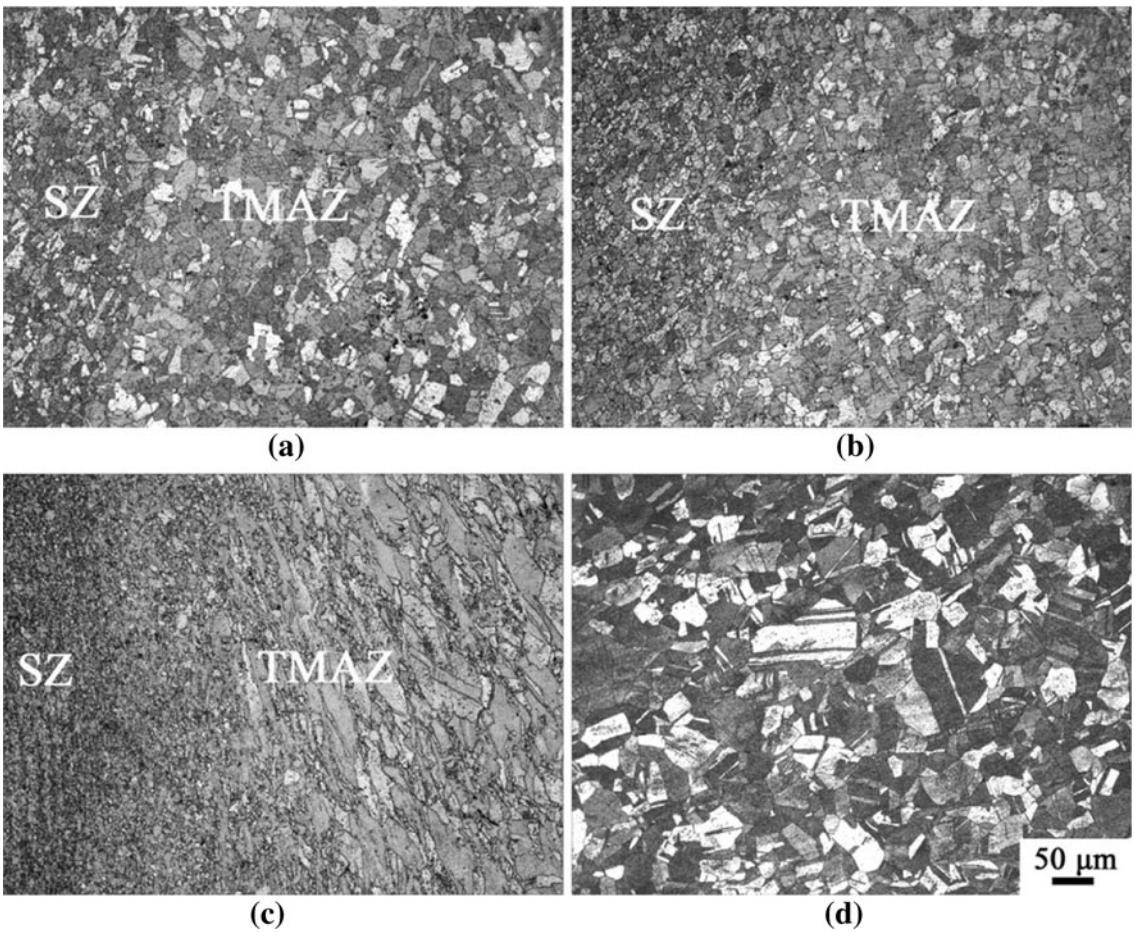

Fig. 4—Microstructures of TMAZ at rotation rate of (*a*) 800 rpm, (*b*) 600 rpm, (*c*) 400 rpm, and (*d*) HAZ at 400 rpm (traverse speed: 50 mm/min).

individual straight boundaries were more frequently discerned (Figure 8(b)). According to the typical selected area diffraction pattern in Figure 8(b), these straight boundaries were the TBs and exhibited the typical twin relationship of {111}/[112] type in copper.

B. *Influence of Heat Input Conditions on Mechanical Properties*

Figure 9 shows the Vicker's hardness profiles along the centerline across the SZ of the FSW copper joints under different welding parameters. In the case of a constant traverse speed of 50 mm/min, at relatively high rotation rates of 600 and 800 rpm, the hardness value of the SZ was lower than that of the PM (Figure 9(a)). Similarly, at the traverse speeds of 50, 100, and 200 mm/min for a constant rotation rate of 800 rpm, the SZ was softer than the PM (Figure 9(b)). However, at a low heat input condition of 400 rpm–50 mm/min, the hardness value of the SZ was significantly higher than that of the PM. As shown in Figure 9(a), a region of ~15 mm in width with lower hardness values (hereafter referred to as the low hardness region) was observed for the FSW joint at 800 rpm–50 mm/min. When the rotation rate

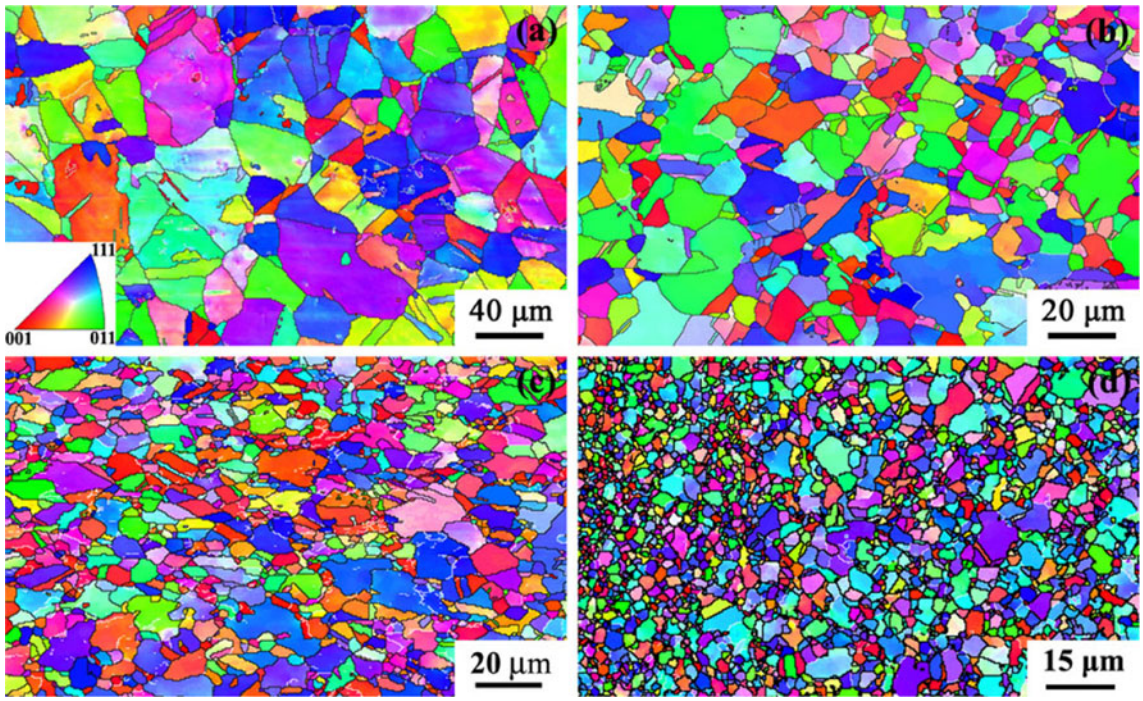

Fig. 5—EBSD orientation maps of (*a*) PM and SZ at (*b*) 800 rpm, (*c*) 600 rpm, and (*d*) 400 rpm (traverse speed: 50 mm/min).

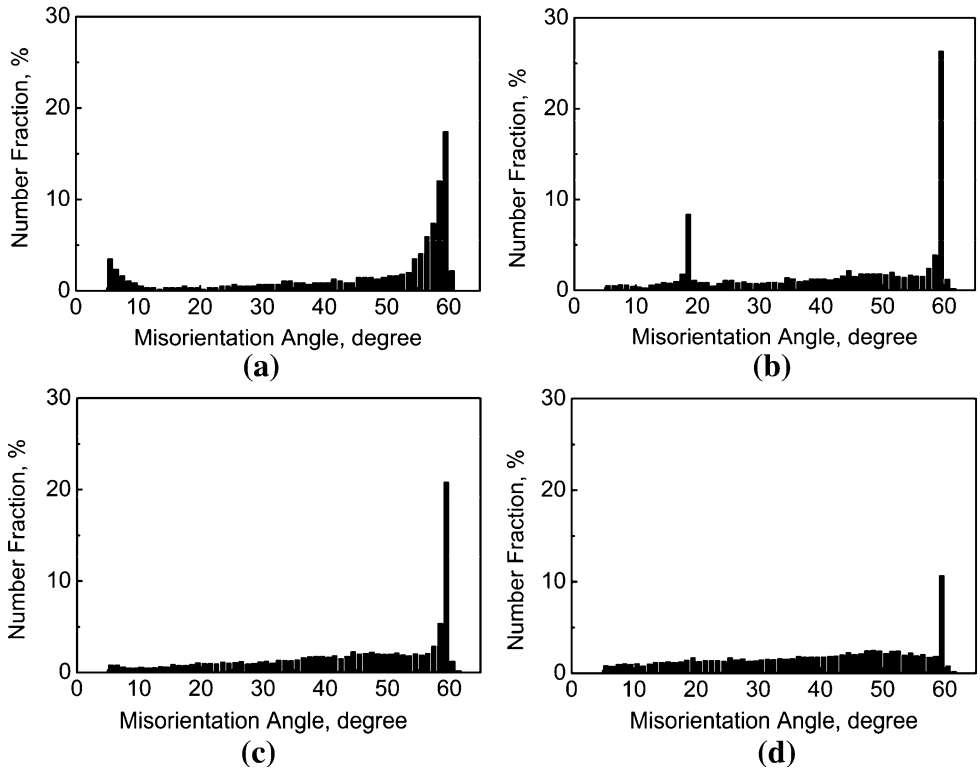

Fig. 6—Grain boundary misorientation angle distributions of (*a*) PM and SZ at (*b*) 800 rpm, (*c*) 600 rpm, and (*d*) 400 rpm (traverse speed: 50 mm/min).

was decreased to 600 rpm, the width of the low hardness region decreased to ~9 mm. At 400 rpm, only the HAZ exhibited low hardness values, and a very narrow low hardness region was observed. Similarly, the low hardness region narrowed steadily as the traverse speed was increased (Figure 9(b)).

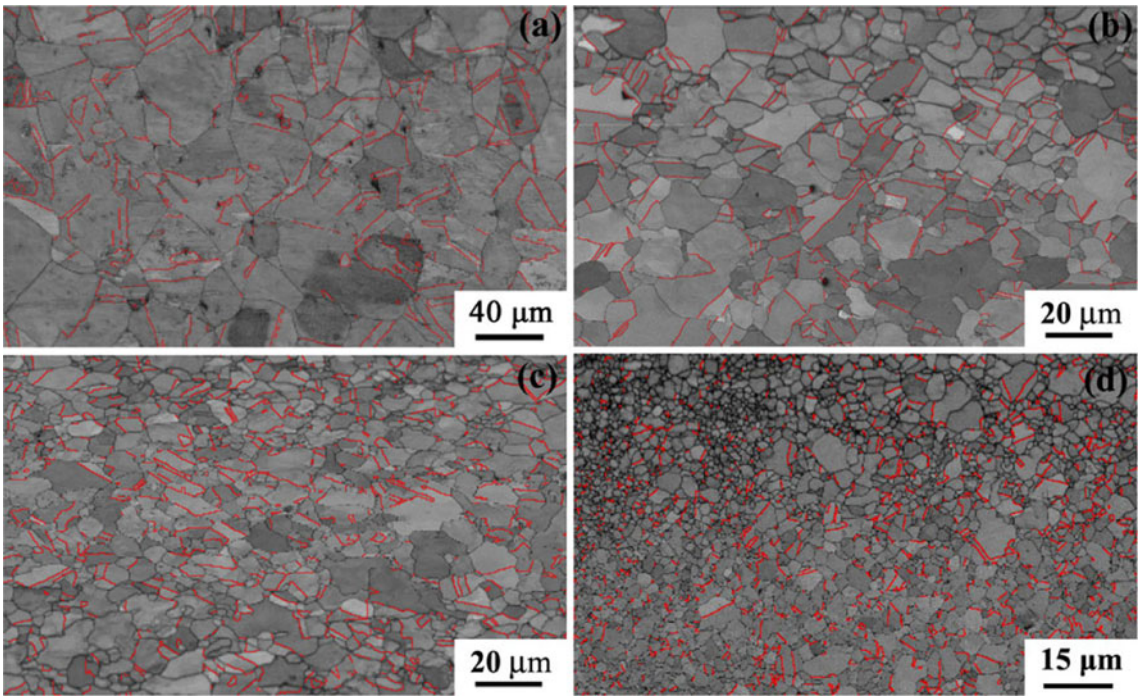

Fig. 7—Distribution of Σ3 boundaries of (*a*) PM and SZ at (*b*) 800 rpm, (*c*) 600 rpm, and (*d*) 400 rpm (transverse speed: 50 mm/min, red lines represent Σ3 boundaries).

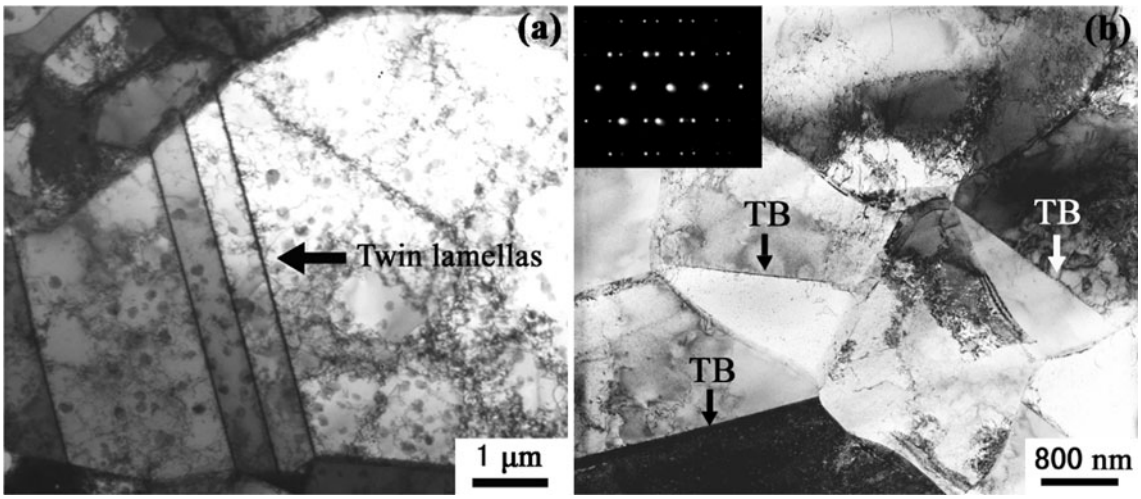

Fig. 8—Typical microstructures of twins at (*a*) 800 rpm and (*b*) 400 rpm (transverse speed: 50 mm/min).

The transverse tensile properties of the PM and the FSW copper joints under various welding parameters are shown in Table I. Compared to the PM, the FSW copper joints exhibited similar ultimate tensile strength (UTS) and decreased yield strength (YS) and elongation. Figures 10(a) and (b) show the variation of the tensile properties with the rotation rates and traverse speeds, respectively. By either decreasing the rotation rate or increasing the traverse speed, *i.e.*, decreasing the heat input, the YS of the welds clearly increased. However, the UTS exhibited only a slight increase. Meanwhile, the elongation tended to decrease as the heat input was decreased.

The fracture of all FSW copper joints occurred at the HAZ with necking, and the plastic deformation remarkably increased as the heat input was increased. Figures 11 and 12 show the top and side views of the failed welds produced at 800, 600, and 400 rpm, respectively. For the joint at a high heat input condition of 800 rpm, relatively uniform deformation occurred within the entire low hardness region (Figures 11(a) and 12(a)). When the rotation rate was decreased to 600 rpm, while plastic deformation was observed within the low hardness region, highly localized plastic deformation occurred at the HAZ (Figures 11(b) and 12(b)). At a low heat input condition of 400 rpm, the plastic

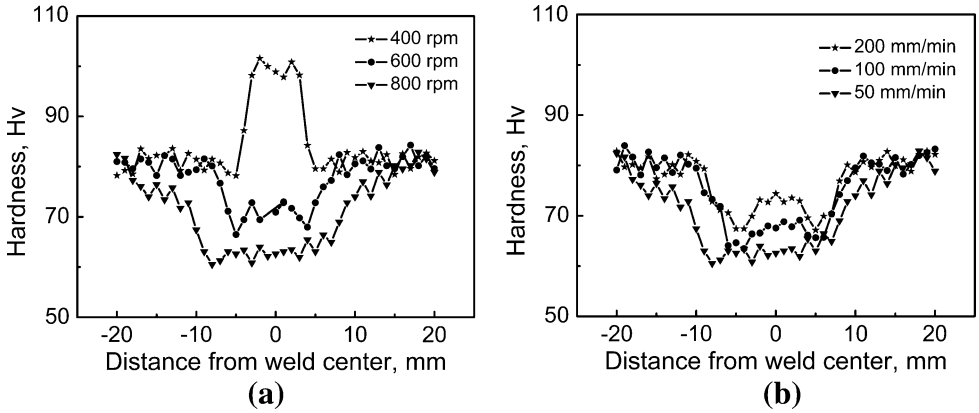

Fig. 9—Hardness profiles in cross sections of welds at (*a*) different rotation rates (traverse speed: 50 mm/min) and (*b*) different traverse speeds (rotation rate: 800 rpm, the advancing side is on the right side).

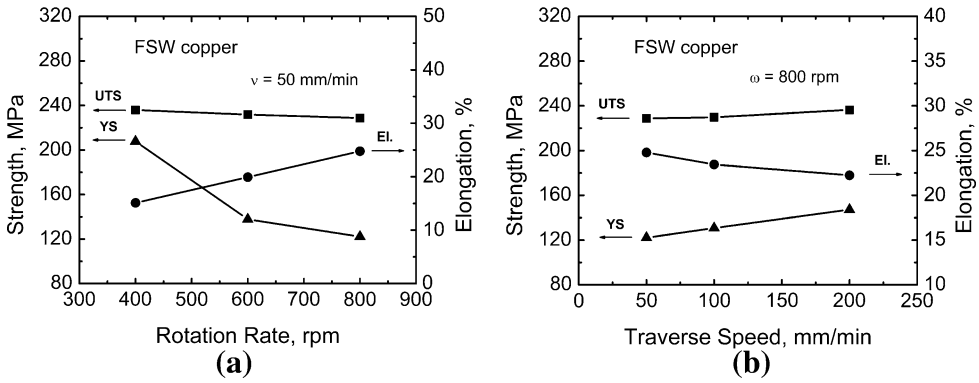

Fig. 10—Transverse tensile properties of FSW copper joints at (*a*) different rotation rates (traverse speed: 50 mm/min) and (*b*) different traverse speeds (rotation rate: 800 rpm).

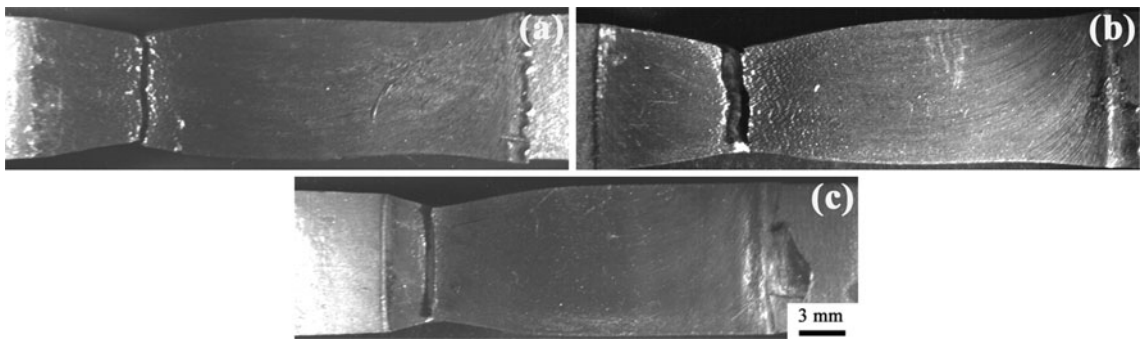

Fig. 11—Top views of failed FSW copper joints under different rotation rates: (*a*) 800 rpm, (*b*) 600 rpm, and (*c*) 400 rpm (traverse speed: 50 mm/min; the advancing side is on the right side).

deformation took place mainly at the narrow HAZ (Figures 11(c) and 12(c)).

IV. DISCUSSION

A. *Microstructural Evolution*

Similar to FSW aluminum alloys,[5] four distinct microstructural zones, *i.e.*, PM, SZ, TMAZ, and HAZ, could be identified in the FSW copper joints (Figure 2). The SZ of the FSW copper joints had a clear outline at the lower heat input conditions of 400 rpm–50 mm/min and 800 rpm–200 mm/min, but the outline became unclear for the joints at higher heat input conditions of 600 rpm–50 mm/min, 800 rpm–50 mm/min, and 800 rpm–100 mm/min. The discrepancy reflected significantly different microstructures in the SZ and TMAZ produced at various FSW parameters. As will be discussed later, the unclear outline of the SZ at the

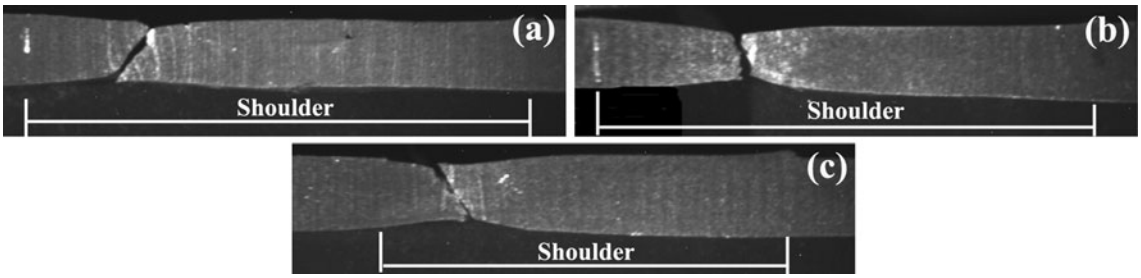

Fig. 12—Side views of failed FSW copper joints under different rotation rates: (*a*) 800 rpm, (*b*) 600 rpm, and (*c*) 400 rpm (traverse speed: 50 mm/min; the advancing side is on the right side).

higher heat input conditions is due to the occurrence of recrystallization in the TMAZ.

In the SZ, the intense plastic deformation and thermal exposure resulted in the occurrence of DRX, thereby producing the remarkable microstructural refinement.[5,14] Figures 3 and 5 indicated that the grain size of the SZ decreased as the rotation rate was decreased or the traverse speed was increased, *i.e.*, as the heat input was reduced. Okamoto *et al.*[8] and Lee *et al.*[9] reported that the average grain size in the SZ of the FSW pure copper joints was 70 to 100 μm, which was associated with higher heat input used in their studies. The present study clearly indicates that the grains of the FSW copper joints can be significantly refined in lower heat input conditions. It is clear from Figure 3 and Table I that grain refining through increasing the traverse speed was not as effective as that through decreasing the rotation rate. Usually, the heat input (thermal cycle) was closely related to the peak temperature and the time, which were mainly determined by the rotation rate and the traverse speed, respectively.[15,17] According to Sato *et al.*,[17] the recrystallized grain size in the SZ increased exponentially with the peak temperature and linearly with time, so the peak temperature exerted the dominant influence. Moreover, Reynolds *et al.*[16] suggested that the weld power (input torque × rotation rate) determined the peak temperature. The general trend toward higher weld power with higher rotation rate was found in their study, and this trend was stronger at lower rotation rates. Therefore, the rotation rate rather than the traverse speed was the dominant parameter in determining the grain size in the SZ during FSW of copper in this study.

The TMAZ is a unique transition zone between the SZ and the HAZ in FSW, and is usually characterized by highly deformed structure in the joints of aluminum alloys.[5] However, previous studies indicated that the TMAZ occurred only at very low heat input conditions for FSW copper joints, and no TMAZ was observed at high heat input conditions.[9,10] In this study, the grains were elongated along the flow lines at lower heat input condition of 400 rpm–50 mm/min. No distinct TMAZ characteristic was observed at higher heat input conditions of 600 and 800 rpm–50 mm/min (Figure 4). Instead, the TMAZ under higher heat input conditions exhibited equiaxed recrystallized microstructure, and the outline around the SZ became unclear due to the small difference in the grain size between the SZ and the TMAZ. From previous studies[9,10] and our observation, the TMAZ was greatly influenced by the heat input conditions. During FSW, the TMAZ experienced combined thermal and mechanical effects. For FSW copper, at lower heat input condition, the grains were elongated under the mechanical action of the pin at a low temperature, so the typical TMAZ microstructure would be obtained. When the heat input was higher, DRX occurred under the strong thermomechanical effect in the TMAZ, producing equiaxed recrystallized grains. As the heat input was increased, the recrystallized grains in the TMAZ increased in size, and were comparable to those in the SZ and HAZ. In this case, the TMAZ could not be clearly distinguished (Figure 2(a)). This may be the reason that no TMAZ was observed at high heat input conditions in the studies of Lee *et al.*[9] and Hautala *et al.*[10]

Compared with those in the PM, the grains in the HAZ grew a little, as shown in Figure 4(d) and Table I. Moreover, the grain size increased slightly in the HAZ as the heat inputs were increased in this study. Liu *et al.*[12] also found that the grain size changed little as the rotation rate was increased from 300 to 800 rpm at a traverse speed of 100 mm/min. These observations suggested that the HAZ changed little in the grain size at relatively low heat input conditions.

Grain boundary characteristics have significant meaning for investigating the recrystallization and superplasticity mechanisms.[18–22] It was reported that the percentage of the HAGBs in the SZ of FSW aluminum alloys was higher than in that processed by conventional thermal working techniques.[18] Liu *et al.*[19] indicated that for FSW cold-rolled 1050 aluminum alloy, the percentages of the HAGBs of the PM and the SZ were 32 and 70 pct, respectively. Mishra and Mahoney,[20] Norman *et al.*,[21] and Liu *et al.*[22] reported that in the SZ of FSW aluminum alloys, the percentage of the HAGBs is 85 to 97 pct. In this study, the percentages of the HAGBs in the SZ at the rotation rate of 800, 600, and 400 rpm were 94.5, 93.9, and 90.3 pct, respectively (Figures 6(b) through (d)). These values were higher than that in fine-grained coppers prepared by SPD, such as equal-channel angular pressed (ECAP) copper, in which the fraction of the HAGBs was ~70 pct after 20 passes.[23] Furthermore, the percentage of the HAGBs increased slightly when the rotation rate was increased. This observation was consistent with that of the FSW 6063 aluminum alloy produced by Sato *et al.*[24] They

reported that the percentage of the HAGBs at 1220 and 2450 rpm was higher than that at 800 rpm. They suggested that part of the LAGBs transformed to the HAGBs during the growth of recrystallized grains under higher heat input.

It is clear from Figures 6 through 8 that the percentage and microstructure of the Σ3 boundaries in the SZ varied greatly at different heat input conditions. In the SZ, after the DRX was finished, grains started to grow, accompanied by twin formation and evolution.[25] From the observed grain sizes for various welding conditions, it is clear that grains grew significantly at higher heat input conditions. Twin formation and evolution during grain growth have been widely studied before, and an acceptable mechanism model based on energy criterion is shown in Figure 13.[25] In Figure 13(a), the grain grows by the triple point between grains A, B, and C moving vertically. As growth proceeds, a growth fault may occur at some point, leading to the formation of a corner grain (T), which is a twin of grain A (Figure 13(b)). Because the energy of the coherent twin boundary AT is very low (24 mJ m^{-2}) compared to that of the general HAGBs (625 mJ m^{-2}),[26] there may be a reduction in total boundary energy, and therefore the twin configuration will be stable and grow. This condition, in two dimensions, is

$$\gamma_{AT}L_{13} + \gamma_{TC}L_{23} + \gamma_{TB}L_{12} < \gamma_{AC}L_{23} + \gamma_{AB}L_{12} \quad [1]$$

where γ_{ij} is the energy of the boundary between grains i and j, and L_{xy} is the distance between points x and y. The growth will be terminated if the triple point ABC reacts with another triple point such as BCE, resulting in a grain configuration with a less favorable energy balance (Figure 13(c)). In such a model, as the grain growth proceeds, the number of twin lamellas increases and new corner twin forms continuously. Therefore, at high heat input conditions, the percentage of TBs and the number of twin lamellas were quite high, as shown in Figures 6 through 8. At a very low heat input of 400 rpm–50 mm/min, TBs existed mainly by corner twins, as shown in Figure 13(b), and the percentage was less than that under the higher heat input conditions. Therefore, the heat input condition exerted a significant effect on the process of grain growth, which decided the number and microstructure of the TBs. As the heat input was decreased, the fraction of the twins decreased and the number of the twin lamellas was reduced.

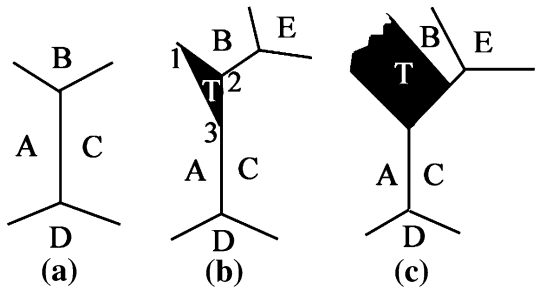

Fig. 13—Mechanism for twin formation and evolution during grain growth process.[25]

B. *Mechanical Properties*

In our previous work, we reported that the hardness values of the PM and the SZ at 800, 600, and 400 rpm for 50 mm/min were 82.2, 63.1, 72.8, and 99.6 HV, respectively.[11] The hardness profiles along the mid-thickness of the welds further proved that the hardness values in the SZ increased as the rotation rate was decreased or as the traverse speed was increased (Figure 9). At the HAZ, the thermal exposure resulted in both grain coarsening and softening as a result of annealing. Therefore, the HAZ was the softest region for all the FSW copper joints, as shown in Figure 9.

The as-received copper in this study is in the 1/2H condition. Therefore, the FSW produced two competitive factors influencing the hardness of the SZ. The thermal exposure resulted in remarkable softening effect, thereby reducing the hardness of the SZ. However, the significant grain refinement resulting from FSW increased the hardness of the SZ. At higher heat input conditions of 600 and 800 rpm for 50 mm/min and of 100 and 200 mm/min for 800 rpm, the softening effect was dominant. Therefore, the hardness values of the SZ were lower than those of the PM and a wide low hardness region was observed. With increasing the FSW heat input, the low hardness region widened, as shown in Figure 9. Furthermore, the hardness profile and the lowest hardness value of the FSW copper joint produced at 800 rpm and 50 mm/min in this study are similar to those reported by Hautala *et al.*[10] At a very low heat input condition of 400 rpm–50 mm/min, the grain refinement was dominant, so the hardness values of the SZ were higher than those of the PM and a very narrow HAZ was observed.

Compared to the PM, the as-FSW copper joints produced at various FSW parameters exhibited similar UTS and decreased YS and elongation-to-failure (Table I and Figure 10). For a constant traverse speed of 50 mm/min, the YS values of the FSW joints at 800, 600, and 400 rpm were 55, 62, and 93 pct of the PM and the elongation reached 89, 72, and 55 pct of the PM, respectively. At a constant rotation rate of 800 rpm, the YS values of the FSW joints at 50, 100, and 200 mm/min were 55, 59, and 66 pct of the PM and the elongations were 89, 85, and 80 pct of the PM, respectively. As the heat input was decreased, the YS of the welds increased, and the elongation decreased. Lee *et al.*[9] reported that the transverse UTS of the FSW copper joint reached about 87 pct of the PM. Hautala *et al.*[10] pointed out that at 800 rpm and 250 mm/min, the UTS and elongation of the FSW copper joint were 95 and 47 pct of the PM, respectively. Okamoto *et al.*[8] reported that at 1300 rpm and 170 mm/min, the UTS of the FSW copper joint was slightly lower than that of the PM (with 1/4H) and its elongation was higher than that of the PM, but the YS was reduced to about 50 pct of the PM. Reduced YS of the FSW copper joints was associated with the high heat input used in their works.

For the present FSW copper joints, while the UTS was fundamentally independent of the heat input conditions, the practically important YS was significantly influenced by the heat input conditions. By

comparing the present study with other investigations, sound FSW copper joints with excellent mechanical properties can be produced at low heat input conditions. For example, at a low heat input of 400 rpm and 50 mm/min, the UTS, YS, and elongation-to-failure of the weld reached 99, 93, and 55 pct of the PM, respectively.

Figures 11 and 12 reveal that the joints failed at the HAZ with the lowest hardness, indicating that the fracture location of the welds was consistent with the lowest hardness zone (Figure 9). Previously, Okamoto *et al.*[8] reported that the fracture of the FSW copper joint at 1300 rpm and 170 mm/min occurred at the HAZ with the lowest hardness. Similarly, Lee *et al.*[9] also found that at 1250 rpm and 61 mm/min, the fracture of the FSW copper joint occurred at the HAZ, which showed the lowest hardness. Figure 14 shows the variation of the YS of the FSW copper joints with the lowest hardness value of the HAZ. It is clear that the YS of the FSW copper joints increased linearly as the lowest hardness value of the HAZ increased. Similarly, Sato and Kokawa[27] also found that the YS was roughly proportional to the minimum hardness in the FSW 6063 aluminum joints. Considering the inhomogeneous microstructure of the transverse tensile specimen, the global YS of the welded joint should be governed by the weakest region.[5,27] In this study, the HAZ with the lowest hardness values was the weakest region of the FSW copper joint. The initial state of the PM used in this study was 1/2H, so many dislocation walls, tangles, cell walls, or subgrain boundaries existed in the PM, and this caused the high YS of the PM. During FSW, the HAZ experienced a thermal cycle, which caused an annealing effect. Then the HAZ was softened because various dislocation structures were reduced and the grains were coarsened during the thermal cycle. Based on the preceding discussion, to obtain the FSW copper joints with higher strength, it is necessary to decrease the heat input of FSW to reduce the annealing effect.

Figures 9, 11, and 12 reveal that the FSW parameters exerted a significant effect on the width of the low hardness region, thereby influencing the plastic deformation behavior and the ductility of the FSW copper joints. For the joint produced at a higher heat input of 800 rpm–50 mm/min, because of the relatively uniform hardness distribution within the low hardness region, as shown in Figure 9, a relatively uniform plastic deformation took place within this region with necking occurred (Figures 11(a) and 12(a)). As the heat input was decreased to 600 rpm–50 mm/min, the low hardness region narrowed and the HAZ with the lowest hardness value became obvious (Figure 9(a)). In this case, although the plastic deformation occurred within the whole low hardness region, highly localized plastic deformation was observed at the HAZ with an obvious necking (Figures 11(b) and 12(b)). At a very low heat input of 400 rpm–50 mm/min, the hardness of only the HAZ was lower than that of the PM (Figure 9). Then, the plastic deformation occurred mainly at the HAZ with an obvious localized necking (Figures 11(c) and 12(c)). The results of Sato and Kokawa[27] showed that the tensile strain distribution of FSW joints was inhomogeneous, and local strains caused the low elongation. As the heat input conditions were decreased, the localized plastic deformation became more and more obvious, as shown in Figures 11 and 12, and this caused the decrease of the elongation (Table I). Therefore, the lowest elongation was obtained at the low heat input of 400 rpm–50 mm/min because of the local strains in the narrow HAZ.

The overall implication of the presented results is significant. It is indicated that under relatively low heat input conditions, defect-free FSW copper joints can be successfully produced. By changing the heat input conditions, the microstructure and mechanical properties of the welds can be tailormade. At lower heat input condition, the FSW copper joints with better mechanical properties can be obtained. This indicates that FSW is an effective method to join pure copper and will find increasing industrial applications.

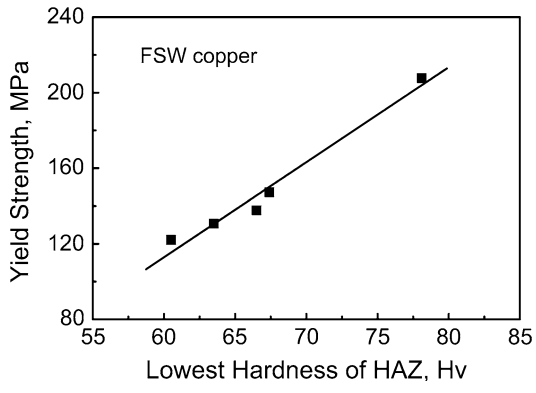

Fig. 14—Variation of YS of FSW copper joints with lowest hardness values of HAZ.

V. CONCLUSIONS

1. Under relatively low heat input conditions with a rotation rate of 400 to 800 rpm and a traverse speed of 50 to 200 mm/min, sound FSW copper joints 5 mm in thickness were obtained.
2. The grain size of the SZ under various parameters was smaller than that of the PM and decreased as the heat input conditions were decreased. A higher percentage of the HAGB (90.2 to 94.5 pct) was observed in the SZ, and the percentage increased as the heat input was increased. When the heat input was reduced, the fraction of the twins and the number of the twin lamellas were reduced.
3. Under higher heat input conditions of 600 and 800 rpm for 50 mm/min, the TMAZ exhibited equiaxed recrystallized grain structure. As the heat input condition was decreased to 400 rpm–50 mm/min, the typical characteristics of the TMAZ with elongated grains could be discerned. The grains were slightly coarsened in the HAZ compared to the PM, and the grain size changed little under various parameters.

4. Under higher heat input conditions of 600 rpm for 50 mm/min and 800 rpm for 50 to 200 mm/min, the hardness values of the SZ were lower than that of the PM, whereas at a very low heat input condition of 400 rpm for 50 mm/min, the hardness value of the SZ was higher than that of the PM. As the heat input conditions were decreased, the hardness of the SZ increased and the width of the low hardness region narrowed.
5. The fracture occurred at the HAZs for all the FSW copper joints, and the UTS was similar to that of the PM. However, the YS and elongation were lower than those of the PM. As heat input conditions were decreased, the YS increased significantly. Simultaneously, the elongation decreased due to the enhanced strain localization.

ACKNOWLEDGMENTS

This work was supported by the National Outstanding Young Scientist Foundation under Grant No. 50525103, the National Basic Research Program of China under Grant No. 2006CB605205, and the Hundred Talents Program of Chinese Academy of Sciences.

REFERENCES

1. Chinese Welding Society: *Welding Handbook*, 2nd ed., China Machine Press, Beijing, 2001, vol. 2, pp. 608–43.
2. S.A. Fabritsiev, A.S. Pokrovsky, M. Nakamichi, and H. Kawamura: *J. Nucl. Mater.*, 1998, vol. 2030, pp. 258–63.
3. T.D. Uzunov, S.P. Stojanov, and S.I. Lambov: *Vacuum*, 1999, vol. 52, pp. 365–68.
4. W.M. Thomas, E.D. Nicholas, J.C. Needham, M.G. Murch, P. Templesmith, and C.J. Dawes: G.B. Patent Application No. 9125978.8, Dec. 1991.
5. R.S. Mishra and Z.Y. Ma: *Mater. Sci. Eng. R*, 2005, vol. 50, pp. 1–78.
6. C.G. Andersson and R.E. Andrews: *Proc. 1st Int. Symp. on Friction Stir Welding*, Thousand Oaks, CA, 1999.
7. C.G. Andersson, R.E. Andrews, B.G.I. Dance, M.J. Russell, E.J. Olden, and R.M. Sanderson: *Proc. 2nd Int. Symp. on Friction Stir Welding*, Gothenburg, Sweden, 2000.
8. K. Okamoto, M. Doi, S. Hirano, K. Aota, H. Okamura, Y. Aono, and T.C. Ping: *Proc. 3rd Int. Symp. on Friction Stir Welding*, Kobe, Japan, 2001.
9. W.B. Lee and S.B. Jung: *Mater. Lett.*, 2004, vol. 58, pp. 1041–46.
10. T. Hautala and T. Tiainen: *Proc. 6th Int. Conf. on Trends in Welding Research*, Pine Mountain, GA, 2003, ASM INTERNATIONAL, Materials Park, OH, 2003, pp. 324–28.
11. G.M. Xie, Z.Y. Ma, and L. Geng: *Scripta Mater.*, 2007, vol. 57, pp. 73–76.
12. H.J. Liu, J.J. Shen, Y.X. Huang, L.Y. Kuang, C. Liu, and C. Li: *Sci. Technol. Weld. Join.*, 2009, vol. 14, pp. 577–83.
13. T. Sakthivel and J. Mukhopadhyay: *J. Mater. Sci.*, 2007, vol. 42, pp. 8126–29.
14. T.R. McNelley, S. Swaminathan, and J.Q. Su: *Scripta Mater.*, 2008, vol. 58, pp. 349–54.
15. A.P. Reynolds: *Mater. Sci. Forum*, 2007, vols. 539–543, pp. 207–14.
16. A.P. Reynolds, W. Tang, Z. Khandkar, J.A. Khan, and K. Lindner: *Sci. Technol. Weld. Join.*, 2005, vol. 10, pp. 190–99.
17. Y.S. Sato, M. Urata, and H. Kokawa: *Metall. Mater. Trans. A*, 2002, vol. 33A, pp. 625–35.
18. Z.Y. Ma, R.S. Mishra, M.W. Mahoney, and R. Grimes: *Metall. Mater. Trans. A*, 2005, vol. 36A, pp. 1447–58.
19. L. Liu, H. Nakayama, S. Fukumoto, A. Yamamoto, and H. Tsubakino: *Mater. Trans. JIM*, 2004, vol. 8, pp. 2665–68.
20. R.S. Mishra and M.W. Mahoney: *Mater. Sci. Forum*, 2001, vols. 357–359, pp. 507–12.
21. A.F. Norman, I. Brough, and P.B. Prangnell: *Mater. Sci. Forum*, 2000, vols. 331–337, pp. 1713–18.
22. F.C. Liu, Z.Y. Ma, and L.Q. Chen: *Scripta Mater.*, 2009, vol. 60, pp. 968–71.
23. A. Vinogradov, T. Suzuki, S. Hashimoto, K. Kitagawa, A. Kuznetsov, and S. Dobatkin: *Mater. Sci. Forum*, 2006, vols. 503–504, pp. 971–76.
24. Y.S. Sato, H. Kokawa, M. Enomoto, and S. Jogan: *Metall. Mater. Trans. A*, 1999, vol. 30A, pp. 2429–37.
25. F.J. Humphreys and M. Hatherly: *Recrystallization and Related Annealing Phenomena*, 2nd ed., Elsevier Ltd, New York, NY, 2004, pp. 261–67.
26. L.E. Murr: *Interfacial Phenomena in Metals and Alloys*, Addison-Wesley, Reading, MA, 1975, p. 131.
27. Y.S. Sato and H. Kokawa: *Metall. Mater. Trans. A*, 2001, vol. 32A, pp. 3023–31.